

Real-time distance measurement immune from atmospheric parameters using optical frequency combs

Pu Jian¹, Olivier Pinel^{1,2}, Claude Fabre¹, Brahim Lamine¹ and
Nicolas Treps^{1,*}

¹ Laboratoire Kastler Brossel, Université Pierre et Marie Curie–Paris 6, ENS, CNRS; 4 place
Jussieu, 75252 Paris, France

² Centre for Quantum Computation and Communication Technology, Department of Quantum
Science, The Australian National University, Canberra, ACT 0200, Australia

[*nicolas.treps@upmc.fr](mailto:nicolas.treps@upmc.fr)

Abstract: We propose a direct and real-time ranging scheme using an optical frequency combs, able to compensate optically for index of refraction variations due to atmospheric parameters. This scheme could be useful for applications requiring stringent precision over a long distance in air, a situation where dispersion becomes the main limitation. The key ingredient is the use of a mode-locked laser as a precise source for multi-wavelength interferometry in a homodyne detection scheme. By shaping temporally the local oscillator, one can directly access the desired parameter (distance) while being insensitive to fluctuations induced by parameters of the environment such as pressure, temperature, humidity and CO₂ content.

© 2012 Optical Society of America

OCIS codes: (120.2920) Homodyning; (140.4050) Mode-locked lasers; (280.3400) Laser range finder; (320.5540) Pulse shaping

References and links

1. A. Weiss, M. Hennes, and M. Rotach, “Derivation of refractive index and temperature gradients from optical scintillometry to correct atmospherically induced errors for highly precise geodetic measurements,” *Surveys in geophysics* **22**, 589–596 (2001).
2. P. Exertier, P. Bonnefond, F. Deleflie, F. Barlier, M. Kasser, R. Biancale, and Y. MÈnard, “Contribution of laser ranging to earth’s sciences,” *Comptes Rendus Geoscience* **338**, 958 – 967 (2006).
3. K. Djerroud, O. Acef, A. Clairon, P. Lemonde, C. N. Man, E. Samain, and P. Wolf, “Coherent optical link through the turbulent atmosphere,” *Optics Letters* **35**, 1479–1481 (2010).
4. F. Delplancke, “The prima facility phase-referenced imaging and micro-arcsecond astrometry,” *New Astronomy Reviews* **52**, 199 – 207 (2008).
5. M. Cui, R. N. Schouten, N. Bhattacharya, and S. A. Berg, “Experimental demonstration of distance measurement with a femtosecond frequency comb laser,” *Journal of European Optical Society Rapid Publications* **3**, 08003 (2008).
6. B. Lamine, C. Fabre, and N. Treps, “Quantum improvement of time transfer between remote clocks,” *Physical Review Letters* **101**, 123601 (2008).
7. J. Ye, “Absolute measurement of a long, arbitrary distance to less than an optical fringe,” *Optics letters* **29**, 1153–1155 (2004).
8. P. L. Bender and J. C. Owen, “Correction of optical distance measurement for the fluctuating atmospheric index of refraction,” *Journal of geophysical research* **70**, 2461–2462 (1965).
9. C. Helstrom, “The minimum variance of estimates in quantum signal detection,” *Information Theory, IEEE Transactions on* **14**, 234 – 242 (1968).

10. S. Braunstein and C. Caves, "Statistical distance and the geometry of quantum states," *Physical Review Letters* **72**, 3439–3443 (1994).
11. O. Pinel, J. Fade, D. Braun, P. Jian, N. Treps, and C. Fabre, "Ultimate sensitivity of precision measurements with intense Gaussian quantum light: A multimodal approach," *Physical Review A* **85**, 1–4 (2012).
12. H. Matsumoto and T. Honda, "High-accuracy length-measuring interferometer using the two-colour method of compensating for the refractive index of air," *Measurement Science and Technology* **3**, 1084–1086 (1992).
13. K. Meiners-Hagen and A. Abou-Zeid, "Refractive index determination in length measurement by two-colour interferometry," *Measurement Science and Technology* **19**, 084004–+ (2008).
14. A. N. Golubev and A. M. Chekhovsky, "Three-color optical range finding," *Applied Optics* **33**, 7511–7517 (1994).
15. P. Réfrégier, *Noise theory and application to physics: from fluctuations to information* (Springer Verlag, 2004).
16. V. Delaubert, N. Treps, C. Harb, P. Lam, and H. Bachor, "Quantum measurements of spatial conjugate variables: displacement and tilt of a gaussian beam," *Optics letters* **31**, 1537–1539 (2006).
17. M. Hsu, V. Delaubert, P. Lam, and W. Bowen, "Optimal optical measurement of small displacements," *Journal of Optics B: Quantum and Semiclassical Optics* **6**, 495 (2004).
18. B. Edlén, "The Refractive Index of Air," *Metrologia* **2**, 71–80 (1966).
19. P. E. Ciddor, "Refractive index of air: new equations for the visible and near infrared," *Applied Optics* **35**, 1566–+ (1996).
20. G. Bönsch and E. Potulski, "Measurement of the refractive index of air and comparison with modified Edlén's formulae," *Metrologia* **35**, 133–+ (1998).
21. A. Ishida, "Two-wavelength displacement-measuring interferometer using second-harmonic light to eliminate air-turbulence-induced errors," *Japanese Journal of Applied Physics* **28**, L473–L475 (1989).
22. V. Giovannetti, S. Lloyd, and L. Maccone, "Quantum-enhanced measurements: beating the standard quantum limit," *Science* **306**, 1330 (2004).
23. J. C. Owens, "Optical refractive index of air: dependence on pressure, temperature, and composition," *Applied Optics* **6**, 51–+ (1967).
24. E. R. Peck and K. Reeder, "Dispersion of Air," *Journal of the Optical Society of America* (1917-1983) **62**, 958–+ (1972).
25. K. P. Birch and M. J. Downs, "An Updated Edlén Equation for the Refractive Index of Air," *Metrologia* **30**, 155–162 (1993).
26. K. P. Birch and M. J. Downs, "LETTER TO THE EDITOR: Correction to the Updated Edlén Equation for the Refractive Index of Air," *Metrologia* **31**, 315–316 (1994).
27. R. Macovez, M. Mariano, S. D. Finizio, and J. Martorell, "Measurement of the dispersion of air and of refractive index anomalies by wavelength-dependent nonlinear interferometry," *Optics Express* **17**, 13881–13888 (2009).

The accuracy of precise length measurements is commonly limited by dispersive effects. For instance, the dispersion of air is a crucial issue for geodetic surveying [1] or for the optical link between a ground station and a satellite [2]. The lack of knowledge about atmospheric parameters can then act as the main limitation to optical length measurements.

Numerous groups around the world tackle this issue of long range distance measurement. For instance, in atmospheric links such as satellite ranging or Lunar Laser Range, the accuracy provided by time-of-flight measurements reaches the millimeter level or below [2, 3]. Interferometric distance measurements lead to potentially increased accuracies. However, for simple interferometric experiments, the periodicity of the signal results is ambiguous up to an absolute distance of a half-wavelength. This ambiguity distance can be extended by combining signals from multiple wavelengths. For instance, the Very Large Telescope Interferometer uses dual-field interferometry to reach nanometric accuracy in a 100 m air-filled delay line [4].

It is also possible to combine both time-of-flight and phase measurement to obtain a better sensitivity and an absolute distance measurement. The ideal tool for this is the phase-stabilized mode-locked femtosecond laser which delivers a frequency comb that can be seen as a perfect source for multi-wavelength interferometry [5, 6, 7]. The problem we address here is the way to use this tool in a complex environment, in order to perform a dispersion free measurement. We will more precisely treat the example of distance measurement in air independent of the variation of physical parameters such as pressure, temperature, CO₂ content or humidity.

In a multi-parameter environment, where many physical factors can affect the accuracy of distance measurements, these extra parameters need to be measured and their effects com-

pensated. This is the general strategy of the well-known multicolor schemes [8], which we introduce in the first part of this paper.

In the second part, we derive fundamental limits for optimal measurement schemes (i.e. reaching the Cramér-Rao bound with coherent states [9, 10, 11]) for distance measurements through a dispersive medium, using mode-locked lasers. The technique is based on temporal mode-dependent interferometry. We show that, in contrast to multicolor schemes for instance, only one measurement is necessary whatever the number of parasitic parameters we want to cancel. This is done at the cost of a precise spectral mode shaping of the frequency comb that is used.

We finally propose a general all-optical experimental setup using pulse shaping and homodyne detections to reach the previous limit. Our distance measurement can be made insensitive of the environment parameters such as temperature or pressure. No post-processing is needed to achieve a measurement limited by the laser noise. Another advantage over existing schemes is that mode-locked lasers are remarkable tools for optical measurement because of their intrinsic high stability.

Distance measurement in air : multicolor schemes

Let us start by describing the general technique of multicolor schemes. If one needs to measure a distance in air, the fluctuations of parameters such as pressure or temperature limit the achievable accuracy. The general idea to solve this problem is to perform several measurements at different wavelengths to gain informations about these parameters and compensate the measured length for their variations. For example, in the two-wavelength interferometry (2WI), a given distance L is measured using two wavelengths λ_1 and λ_2 . The two observables L_{ϕ_1} and L_{ϕ_2} deduced from the measurement are such that [8, 12, 13]

$$L_{\phi_1} = n_\phi(\lambda_1)L \quad \text{and} \quad L_{\phi_2} = n_\phi(\lambda_2)L. \quad (1)$$

For dry air (pressure of water vapor $P_w = 0$), one finds

$$L = L_{\phi_1} + \alpha(L_{\phi_1} - L_{\phi_2}) \quad \text{with} \quad \alpha = \frac{K(\lambda_1)}{K(\lambda_2) - K(\lambda_1)}, \quad (2)$$

where $K(\lambda)$ is given in Appendix A, and is calculated from the Edlén model of air. The parameter α is independent from pressure, temperature and CO₂ content of air. The standard quantum limit for a distance measurement is obtained by taking $(\delta L_{\phi_i})^{\text{shot}} = \frac{c}{2\sqrt{N}\alpha_i}$. The sensitivity δL on the distance then strongly depends on the value of α . Typically, for $\lambda_1 = 1064 \mu\text{m}$ and $\lambda_2 = 532 \mu\text{m}$, α is of the order of 60. Hence, for a mean photon number $N = 4 \times 10^{16}$ per wavelength (10 mW power and an integration time of 1 s), one gets

$$(\delta L)_{2WI}^{\text{shot}} \simeq 3 \times 10^{-14} \text{ m}. \quad (3)$$

This is the shot noise limit in distance variation measurement (displacement), but one should note that for an absolute distance characterization (ranging), the precise knowledge of α is the main limitation factor ($\delta\alpha/\alpha \sim 1\%$).

For moist air, one can no longer use Eq. (2). If the pressure of water vapor is unknown or changing over time, it leads to a systematic error (see [13] for a discussion). A solution is then to consider a third wavelength λ_3 [14] and a third measurement L_{ϕ_3} so that

$$L = L_{\phi_1} + \beta(L_{\phi_2} - L_{\phi_1}) + \gamma(L_{\phi_3} - L_{\phi_1}). \quad (4)$$

Expressions of β and γ can be found in [14] and do not depend on pressure, temperature, CO₂ content and humidity. Here again these factors can be large, reducing the sensitivity of

displacement measurement. For a same total number of photons and typical wavelengths, the shot noise limit is now around 10^{-12} m. In addition to this degradation, the three-wavelength scheme is experimentally more involved.

From this example one sees that both the required sensitivity and physical characteristics of the medium conditions on the number of extra parameters one has to take into account. For each of these parameters an additional measurement at a different wavelength is necessary.

1. Efficient measurement through dispersive media

We will now give a more general and systematic approach to this problem. First, we derive general equations for the propagation of light through a dispersive medium whose characteristics depend on external parameters. We then elaborate on the ideas developed in [6, 11] and deal with a very general approach on how to efficiently measure parameters affecting the propagation of a light pulse. We derive fundamental limits imposed by the quantum nature of light. One should note nevertheless that we limit ourselves to the study of coherent states, non-classical quantum states being beyond the scope of this article.

1.1. Propagation in a dispersive medium

We consider the propagation of an electromagnetic field along the z direction in a weakly dispersive medium. Its propagation from a source to a detector can be affected by a given set of parameters $\vec{p} = (p_1, \dots, p_i, \dots)$ that modify the propagation distance L and/or the characteristics of the dispersive medium: these may be environmental parameters such as air pressure, temperature, etc., or a physical displacement of the source (or the detector). Neglecting polarization effects and using the paraxial approximation, we assume the field to be in a single transverse mode (such as a TEM_{00} mode), and thus will not write the transverse dependence of the field. We further assume Fourier-limited pulses (assuming perfect temporal coherence) and write the dispersed field, as seen by the detector, as a scalar field:

$$\mathcal{E}(t, \vec{p}) \equiv \mathcal{E}_0 u(t, \vec{p}), \quad (5)$$

where $u(t, \vec{p})$ is the normalized mean field mode (integrated over the measurement time of the detector) and \mathcal{E}_0 is a normalization constant which depends on the number of photons N .

In the following, it will be more convenient to work in the Fourier space:

$$\mathcal{E}(\omega, \vec{p}) \equiv \int \mathcal{E}(t, \vec{p}) e^{i\omega t} dt, \quad u(\omega, \vec{p}) \equiv \int u(t, \vec{p}) e^{i\omega t} dt. \quad (6)$$

We define ω_0 and $\Delta\omega$ as the mean value and variance of the field:

$$\omega_0 = \int \omega |u(\omega, \vec{p})|^2 d\omega, \quad \Delta\omega^2 = \int (\omega - \omega_0)^2 |u(\omega, \vec{p})|^2 d\omega. \quad (7)$$

Let us consider an input field $\mathcal{E}_i(\omega)$ whose frequency profile is known. For the sake of simplicity, the field is considered Gaussian (the same final result can be reached with a non Gaussian field but it involves more complex calculations). This field propagates on a distance $L(\vec{p})$ through a dispersive medium with a dispersion relation $k(\omega, \vec{p})$ which depends on \vec{p} through the refractive index $n_\phi(\omega, \vec{p})$. In the frequency space, this propagation is characterized by a spectral phase $k(\omega, \vec{p})L(\vec{p})$:

$$\mathcal{E}(\omega, p) = \mathcal{E}_i(\omega) e^{ik(\omega, \vec{p})L(\vec{p})}, \quad k(\omega, \vec{p}) = \frac{n_\phi(\omega, \vec{p})\omega}{c}. \quad (8)$$

In this paper, we neglect any absorption of the medium, i.e. we consider a real refractive index. The previous equation (8) is therefore also valid by replacing fields \mathcal{E} by normalized modes u .

For a weakly dispersive medium, the dispersion relation $k(\omega, \vec{p})$ can be expanded to the second order around the mean frequency ω_0 :

$$\mathcal{E}(\omega, \vec{p}) \approx \mathcal{E}_i(\omega) \exp \left[i \left(\omega_0 t_\phi(\vec{p}) + (\omega - \omega_0) t_g(\vec{p}) + \frac{(\omega - \omega_0)^2}{\omega_0} t_{\text{GVD}}(\vec{p}) \right) \right], \quad (9)$$

where

$$t_\phi(\vec{p}) = n_\phi(\omega_0, \vec{p}) \frac{L(\vec{p})}{c}, \quad (10)$$

$$t_g(\vec{p}) = n_g(\omega_0, \vec{p}) \frac{L(\vec{p})}{c} = (n_\phi(\omega_0, \vec{p}) + \omega_0 n'_\phi(\omega_0, \vec{p})) \frac{L(\vec{p})}{c}, \quad (11)$$

$$t_{\text{GVD}}(\vec{p}) = \omega_0 \left(n'_\phi(\omega_0, \vec{p}) + \frac{\omega_0}{2} n''_\phi(\omega_0, \vec{p}) \right) \frac{L(\vec{p})}{c}. \quad (12)$$

n_g is the group index, and $2 \left(n'_\phi(\omega_0, \vec{p}) + \frac{\omega_0}{2} n''_\phi(\omega_0, \vec{p}) \right)$ corresponds to the Group Velocity Dispersion (GVD).

In the temporal domain, the field $\mathcal{E}(t, p) = e^{-i\omega_0 t} \tilde{\mathcal{E}}(t, p)$, the envelope $\tilde{\mathcal{E}}$ of the field travels at the group velocity $\frac{c}{n_g}$ while the carrier ω_0 moves at the phase velocity $\frac{c}{n_\phi}$; a non zero group velocity dispersion leads to a broadening of the envelope.

Any change of a parameter in \vec{p} that affects the distance $L(\vec{p})$ will contaminate all quantities t_ϕ , t_g and t_{GVD} , as well as any variation of the refractive index of the medium. In Section 2, we show how to uncouple, in air, variation of L from variation due to four different environmental parameters: pressure, temperature, humidity and CO₂ content. Note that a generalization to other environmental parameters can be obtained by expanding equation (9) to higher orders of the spectral phase and applying the methods developed later in the paper. Nevertheless, these 4 parameters are typically the most relevant for air.

1.2. Detection scheme and Cramér-Rao bound

The general problem of estimating a parameter $p_i \in \vec{p}$ encoded in a light beam $\mathcal{E}(\vec{p})$ has been treated in [9, 15]. The ultimate limit of sensitivity in the measurement of p_i is given by the so-called quantum Cramér-Rao bound, which can be computed once we specify the quantum state of the light beam (coherent state, squeezed state, entangled state etc...) [11]. For Gaussian states, this Cramér-Rao bound can be reached experimentally with a balanced homodyne detection scheme, as represented in Figure 1. The general idea is that the homodyne detection signal is proportional to the projection of the input field into the Local Oscillator (LO) mode.

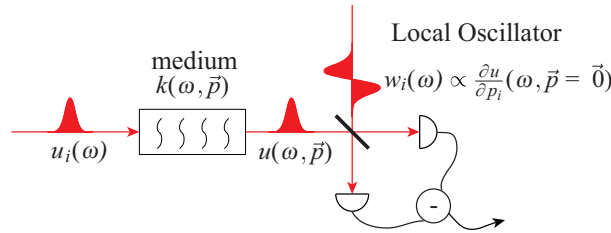


Fig. 1. Detection scheme for measuring p_i at the Cramér-Rao bound.

For a small variation of the set of parameters \vec{p} , the field reads:

$$\mathcal{E}(\omega, \vec{p}) \approx \mathcal{E}(\omega, \vec{0}) + \vec{p} \cdot \vec{\nabla}_{\vec{p}} \mathcal{E}(\omega, \vec{p} = \vec{0}) = \mathcal{E}_0 \left(u(\omega, \vec{0}) + \sum_i p_i K_i w_i(\omega) \right), \quad (13)$$

where w_i are normalized modes such as $w_i(\omega) = \frac{1}{K_i} \frac{\partial u}{\partial p_i}(\omega, \vec{p} = \vec{0})$, and K_i are dimensional normalization constants. Introducing the standard L^2 inner product $\langle f, g \rangle = \int f^*(\omega)g(\omega)d\omega$, one simply has $K_i \equiv \sqrt{\langle \frac{\partial u}{\partial p_i}, \frac{\partial u}{\partial p_i} \rangle}$.

One should note that in general the modes w_i do not form an orthogonal basis. This implies that independent measurements of each parameter become a complex problem that we now discuss in detail extensively. Let us first consider the case where only one parameter $p_i \in \vec{p}$ is influencing the length measurement. It is shown in [16] that in a homodyne detection scheme, if the LO mode is proportional to w_i (and if there is no phase difference between the LO and the signal \mathcal{E}), the detected signal $S[w_i]$ is given by

$$S[w_i] = \frac{1}{K_i} \text{Re}[\langle u(\vec{p}), w_i \rangle]_{p_{j \neq i} = 0} = p_i. \quad (14)$$

For a coherent state illumination with a mean photon number N , the noise in the measurement is $\Delta p_i = 2\sqrt{N}K_i$. Therefore, the smallest p_i that can be measured (i.e. for a signal to noise ratio equal to one, $S/\Delta p = 1$) is given by

$$(p_i)_{\min} = \frac{1}{2\sqrt{N}K_i}. \quad (15)$$

This value coincides with the Cramér-Rao bound with coherent states [11]. This shows that a homodyne detection with a LO shaped in mode w_i defines what is called an efficient measurement of p_i . Moreover, one sees from the previous expression that the sensitivity of the measurement depends both on the number of photons N and on K_i , the latter reflecting the characteristic variation of the mode with the parameter p_i . From now on, the mode w_i will be called the detection mode of the parameter p_i .

An experimental demonstration of the efficiency of such a scheme has been realized for parameters corresponding to spatial displacement of a beam [17, 16], and a theoretical proposition for a time delay through a dispersion-less medium has been made in [6]. One should stress that, generally speaking, these kind of experiments are sensitive to variation of parameters within the detection bandwidth, limited here by light time travel. On the other, this system is immune to any fluctuations, whatever their frequencies, of parameter corresponding to orthogonal modes, given we stay in the linear regime.

Let us now consider the general case where there exists at least another parameter $p_{j \neq i}$ such as w_i and w_j are not orthogonal. In that case, a homodyne detection with LO mode w_i will also be sensitive to p_j . We show here that this issue can be resolved by 'purifying' the detection mode w_i into a new mode w_i^p that is now orthogonal to w_j . This new shape of the LO allows to measure p_i independently of p_j . Nevertheless, because it differs from the detection mode w_i , it leads to a reduced sensitivity in the measurement of p_i . In the general situation, the purified mode for a given parameter p_i is orthogonal to the hyperplane formed by $\{w_{j \neq i}\}$, and the normalization factors are given by $K_i^p = K_i \langle w_i^p, w_i \rangle < K_i$. The sensitivity in the measurement of p_i is therefore decreased and given by $(p_i)_{\min}^p = \frac{1}{2\sqrt{N}K_i^p}$.

The choice for the mode of the LO is an experimental tradeoff between accuracy (no perturbation coming from p_j) and precision. We further elaborate on this point in the following, taking as a simple example the measurement of t_ϕ, t_g and t_{GVD} introduced previously.

To this aim, we introduce a controlled perturbation $p_\phi \ll t_\phi$ of the phase delay $t_\phi \rightarrow t_\phi + p_\phi$, a perturbation $p_g \ll t_g$ of the group delay $t_g \rightarrow t_g + p_g$ and a perturbation $p_{\text{GVD}} \ll t_{\text{GVD}}$ of the group velocity dispersion delay $t_{\text{GVD}} \rightarrow t_{\text{GVD}} + p_{\text{GVD}}$. The corresponding detection modes are

given by:

$$w_\phi(\omega) = iu(\omega) = v_0(\omega) \quad (16)$$

$$w_g(\omega) = i \frac{\omega - \omega_0}{\Delta\omega} u(\omega) = v_1(\omega) \quad (17)$$

$$w_{\text{GVD}}(\omega) = i \frac{1}{\sqrt{3}} \frac{(\omega - \omega_0)^2}{\Delta\omega^2} u(\omega) = \frac{1}{\sqrt{3}} v_0(\omega) + \sqrt{\frac{2}{3}} v_2(\omega) \quad (18)$$

where we have introduced $\{v_i(\omega)\}$ the orthonormal basis of spectral Hermite-Gaussian modes whose expressions are given in Appendix B. The normalization factors are given by $K_\phi = \omega_0$, $K_g = \Delta\omega$ and $K_{\text{GVD}} = \sqrt{3} \frac{\Delta\omega^2}{\omega_0}$.

It is clear that w_ϕ and w_{GVD} are not orthogonal, which implies that a measurement using a LO w_ϕ will not be accurate because of its sensitivity to p_{GVD} , and vice versa. More precisely, measurements over the various detection modes will yield the following signals:

$$S[w_\phi] = p_\phi + \frac{\Delta\omega^2}{\omega_0^2} p_{\text{GVD}} \quad (19)$$

$$S[w_g] = p_g \quad (20)$$

$$S[w_{\text{GVD}}] = \frac{1}{3} \frac{\omega_0^2}{\Delta\omega^2} p_\phi + p_{\text{GVD}}. \quad (21)$$

In order to measure only p_ϕ , one has to consider the *purified mode* w_ϕ^p introduced previously, which is orthogonal to the detection modes of the other parameters. Formally, $w_\phi^p(\omega)$ is orthogonal to the hyperplane generated by $\{w_g, w_{\text{GVD}}\}$ in the vector space $\{w_\phi, w_g, w_{\text{GVD}}\}$ and is given in the present case (up to a scalar factor) by:

$$w_\phi^p(\omega) = \sqrt{\frac{2}{3}} v_0(\omega) - \frac{1}{\sqrt{3}} v_2(\omega). \quad (22)$$

A measurement with LO w_ϕ^p yields:

$$S[w_\phi^p] = p_\phi. \quad (23)$$

Defining $K_\phi^p = K_\phi \langle w_\phi^p, w_\phi \rangle = \sqrt{\frac{2}{3}} \omega_0$, the sensitivity of this measurement is:

$$(p_\phi)_{\min}^p = \frac{1}{2\sqrt{N} \sqrt{\frac{2}{3}} \omega_0}. \quad (24)$$

The two previous equations show that it is possible to retrieve a phase delay information insensitive to any group velocity dispersion fluctuations with only one homodyne measurement. This improvement in accuracy is made at the cost of a decreased precision, determined by the overlap between the purified and non purified modes (here the degradation is given by $\sqrt{3/2}$).

The same process can be applied to obtain the purified mode for measuring p_{GVD} :

$$w_{\text{GVD}}^p(\omega) = v_2(\omega) \quad \text{with} \quad K_{\text{GVD}}^p = \sqrt{2} \frac{\Delta\omega^2}{\omega_0}. \quad (25)$$

The link between the detection modes and the purified modes is shown in Figure 2 and in Table 1.

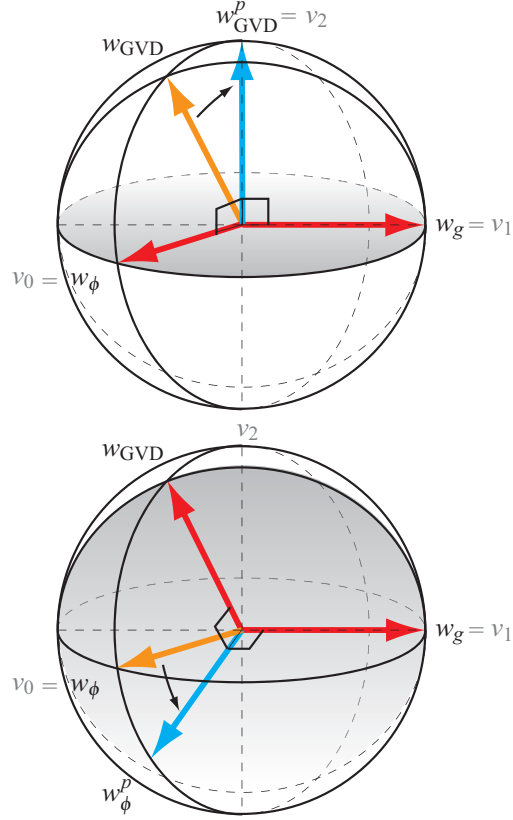


Fig. 2. Relation between the different LO modes in the vector space $\{v_0, v_1, v_2\}$. The modes w_ϕ^p , w_ϕ , w_{GVD} and w_{GVD}^p lie in the same plane.

2. Application to the measurement of a distance in air

Let us now consider the specific case of measuring a distance in air, independently of the fluctuation of environmental parameters such as pressure and temperature. Indeed, induced index refraction fluctuations are the main limitations to precise distance measurement. To access the absolute length, one needs to know precisely the air index variation with these parameters. One solution is to measure precisely these parameters and use an air model to calculate the refractive index, for instance the Edlén [18] or the Ciddor [19] equations. But these techniques are not immune to local variation of the parameters, and some parameters such as the partial pressure of water vapor are very difficult to precisely access. One can also measure directly the local refractive index using a refractometer [20].

Another solution is to make several measurements in order to compensate for these effects. This is the principle of multicolor interferometry [8], whose state of the art is based on second harmonic generation [21, 12], as we have presented in the introduction. Here we develop our new experimental scheme based on mode-locked lasers interferometry as introduced in the previous section. This technique is another kind of multicolor interferometry and allows for direct measurement of distance in air independently of parameters from the environment.


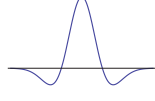
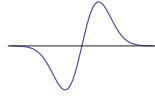
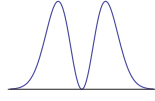
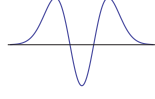
Parameter	Mode	Sensitivity	Temporal profile
p_ϕ	Detection: $w_\phi = v_0$	$\frac{1}{2\sqrt{N}\omega_0}$	
	Purified: $w_\phi^p = \sqrt{\frac{2}{3}}v_0 - \frac{1}{\sqrt{3}}v_2$	$\frac{1}{2\sqrt{N}\sqrt{\frac{2}{3}}\omega_0}$	
p_g	$w_g = v_1$	$\frac{1}{2\sqrt{N}\Delta\omega}$	
p_{GVD}	Detection: $w_{\text{GVD}} = \frac{1}{\sqrt{3}}v_0 + \sqrt{\frac{2}{3}}v_2$	$\frac{1}{2\sqrt{N}} \frac{\omega_0}{\sqrt{3}\Delta\omega^2}$	
	Purified: $w_{\text{GVD}}^p = v_2$	$\frac{1}{2\sqrt{N}} \frac{\omega_0}{\sqrt{2}\Delta\omega^2}$	

Table 1. Summary of the different LO modes and the sensitivities.

2.1. Ranging through air

We apply the technique developed in Section 1.2 to the measurement of the absolute distance L in air. The parameter to be measured with high sensitivity is $p_L = L$. Fluctuations of the environment do perturb this measurement. They can be separated into two groups of parameters. Firstly temperature T , pressure P and CO_2 content x affect air index through the same function, as can be seen in the air model developed in Appendix A. They will be described by only one parameter $p_X = X(T, P, x)$. Secondly, pressure of water vapor P_w has an independent influence, for which we define the parameter $p_{P_w} = P_w$.

One can calculate the corresponding detection modes using the Edlén model of refractive index recalled in the appendix and the second order development of the electric field introduced in the first section. The distance detection mode is given by :

$$w_L(\omega) = \frac{1}{cK_L} (\omega_0 v_0(\omega) + \Delta\omega v_1(\omega)) \quad (26)$$

and the two other detection modes are given in the appendix.

These modes are not linearly independent. Thus if we consider a possible experimental scheme with homodyne detection in the detection mode for L (see Figure 3) the measured signal will be :

$$S[w_L] = p_L + \frac{K_X}{K_L} \langle w_L, w_X \rangle p_X + \frac{K_{P_w}}{K_L} \langle w_L, w_{P_w} \rangle p_{P_w}. \quad (27)$$

Therefore, the signal will be contaminated by variations of the different parameters p_X and p_{P_w} . Let us first compute the shot noise limit in the case where p_X and p_{P_w} are zero (or sufficiently small). To compare with multicolor schemes, in the remainder of this section the measurement is performed using $N = 8 \times 10^{16}$ photons and assuming a laser bandwidth of $\Delta\omega = \frac{\omega_0}{6}$ (corresponding to 3 fs FWHM Fourier-limited pulses). The shot noise limited sensitivity to displacement is about 2×10^{-16} m, comparable to usual interferometric measurement schemes.

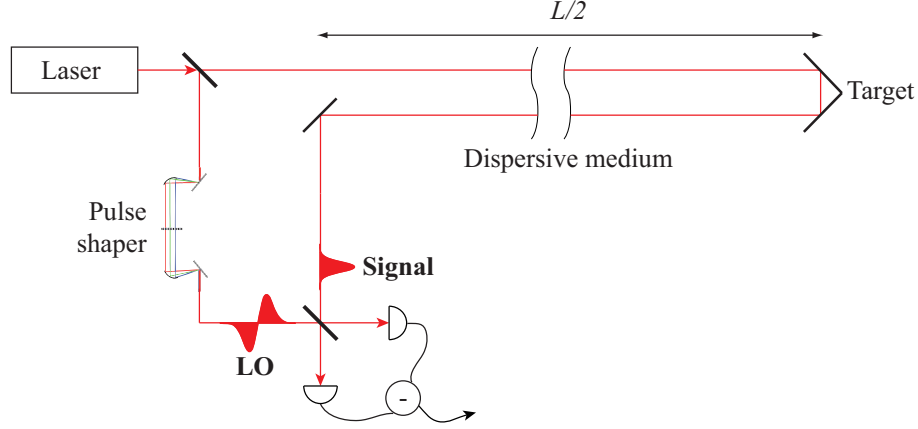


Fig. 3. Direct distance measurement with an appropriately shaped LO.

One can evaluate the contamination from the other parameters calculating the pre-factor of p_X and p_{P_w} in equation (27). One finds $\frac{1}{L} \frac{K_X}{K_L} \langle w_L, w_X \rangle = 27 \times 10^{-5} \text{ Pa}^{-1}$ and $\frac{1}{L} \frac{K_{P_w}}{K_L} \langle w_L, w_{P_w} \rangle = -3.7 \times 10^{-10} \text{ Pa}^{-1}$. These factors are big compared to shot noise limited pure distance measurements. It means it is necessary in this case to take into account the parasitic parameters in order to preserve the accuracy of the measurement. To solve this issue, we can apply the detection mode purification procedure introduced previously :

$$w_L^p(\omega) \propto w_L(\omega) - \frac{\langle w_L, w_{P_w} \rangle - \langle w_X, w_{P_w} \rangle \langle w_L, w_X \rangle}{1 - \langle w_X, w_{P_w} \rangle^2} w_{P_w}(\omega) \quad (28)$$

$$- \frac{\langle w_L, w_X \rangle - \langle w_X, w_{P_w} \rangle \langle w_L, w_{P_w} \rangle}{1 - \langle w_X, w_{P_w} \rangle^2} w_X(\omega) . \quad (29)$$

The spectral profiles of the purified and non-purified modes are plotted in Figure 4. The normalization constant as well as the derivation of this mode can be found in Appendix C. It is found that :

$$K_L^p = K_L \sqrt{1 - \frac{\langle w_L, w_{P_w} \rangle^2 + \langle w_L, w_X \rangle^2 - 2 \langle w_L, w_{P_w} \rangle \langle w_L, w_X \rangle \langle w_X, w_{P_w} \rangle}{1 - \langle w_X, w_{P_w} \rangle^2}} . \quad (30)$$

In that case, the shot noise limit has the following value :

$$(\delta L)_{\text{IHD}}^{\text{shot}} = \frac{c}{2\sqrt{N}K_L^p} = 2 \times 10^{-11} \text{ m} . \quad (31)$$

As a matter of comparison, a purification for p_X only (which would be equivalent to the two-color scheme) leads to a shot noise limit of $(\delta L)_{\text{IHD}}^{\text{shot}} = \frac{c}{2\sqrt{N}K_L^p} = 3 \times 10^{-13} \text{ m}$. Even if the precision is 2 orders of magnitude better, the accuracy of the measurement is not controlled because of the unknown value of humidity introducing a systematic error.

Using that scheme, one can perform a single-shot measurement of distance immune from environmental parameters fluctuations. Sensitivity is of the same order of magnitude than in multicolor scheme (slightly lower in our examples, but this is simply due to smaller spectral width), and depends on how many parameters one wants to get immune from. From a more

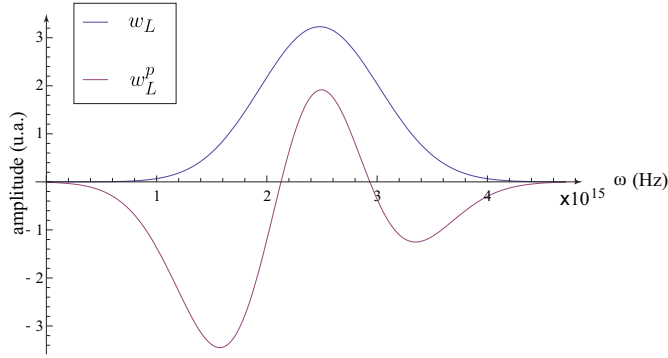


Fig. 4. Spectral profile of modes w_L and w_L^p for 3 fs FWHM Gaussian pulses.

technical point of view, no complex frequency generation is necessary, a femtosecond source is enough to perform the measurement. Furthermore, the scheme described here could be extended to more parameters. Of course, the mode shaping can be more difficult to produce and in particular the precision required in shaping becomes more stringent when more parameters are considered. In a realistic implementation, one can set up active pulse-shaping with search algorithms to determine the proper shaping. It is significant to notice that all the work is to be done at the detection stage and not on the light sent through the medium, which makes it much easier to handle.

3. Conclusion

We have exhibited a novel optimal and all-optical scheme to measure in real time a distance compensated for refractive index changes. It relies on a homodyne detection whose local oscillator projects the measurement on an appropriate mode, hence no post-processing is necessary. We believe this is a simplification compared to existing schemes such as spectral interferometry for example, where derivatives of the spectral phase have to be done after the measurement.

Let us finally mention that this scheme can further be improved in order to go below the standard quantum limit. It is well known that the sensitivity of a measurement can outreach the shot noise limit by using quantum resources such as squeezed or entangled light [22]. In the scheme presented in this paper, this can be achieved by using a multimode signal light beam with squeezing in the detection mode associated to the measurement, as demonstrated in Ref. [11].

A. Index of refraction of air

The common equations used to derive the wavelength dependence of the refractive index of air are given by the Edlén equations [18], modified by different authors since that time [19, 23, 24, 25, 26, 20]. The accuracy of those equations are roughly of the order of a few 10^{-9} for dry air and 10^{-8} for moist air and needs to take into account a large number of parameters, usually temperature, pressure, CO_2 content, pressure of water vapor. Moreover, different studies do not necessarily agree and do not cover the whole spectrum. A recent precise measurement of the refractive index of air has been done in [27]. Experimentally, measuring all those parameters can be difficult for certain situations, and in addition those parameters have to be measured in real time, in order to compensate for fluctuations of the refractive index.

In this paper we consider the updated Edlén formula of Bönsch and Potulski [20] :

$$n_\phi(\sigma, T, P, x, P_w) - 1 = K(\sigma)X(T, P, x) - g(\sigma)P_w \quad (32)$$

where $\sigma = 1/\lambda$ is the wavenumber and

$$K(\sigma) = 10^{-8} \left(A + \frac{B}{130 - \sigma^2} + \frac{C}{38.9 - \sigma^2} \right), \quad (33)$$

$$X(T, P, x) = \frac{P}{D} \frac{1 + 10^{-8}(E - FT)P}{1 + GT} [1 + H(x - 0.04\%)] , \quad (34)$$

$$g(\sigma) = 10^{-10} (I - J\sigma^2), \quad (35)$$

with σ in μm^{-1} , P and P_w in Pascal (Pa), T in degree Celsius ($^\circ\text{C}$) and x , the CO_2 content, in percentage. The different coefficients further read

$$A = 8091.37, \quad B = 2333983, \quad C = 15518, \quad (36)$$

$$D = 932164.60, \quad E = 0.5953, \quad F = 0.009876, \quad G = 0.0036610, \quad (37)$$

$$H = 0.5327, \quad (38)$$

$$I = 3.802, \quad J = 0.0384. \quad (39)$$

The group index is therefore given by

$$n_g(\sigma, T, P, x, P_w) - 1 = (K(\sigma) + \sigma K'(\sigma))X(T, P, x) - (g(\sigma) + \sigma g'(\sigma))P_w, \quad (40)$$

so that $n_g - n_\phi = \sigma (K'(\sigma)X(T, P, x) - g'(\sigma)P_w)$.

B. Hermite-Gaussian set of spectral modes

For a Gaussian mean field mode

$$u(\omega) = \frac{1}{\sqrt{\Delta\omega}} \frac{1}{(2\pi)^{1/4}} e^{-\frac{(\omega - \omega_0)^2}{4\Delta\omega^2}}, \quad (41)$$

we introduce the Hermite-Gauss modes

$$v_n(\omega) = i \frac{1}{\sqrt{2^n n!}} H_n \left(\frac{\omega - \omega_0}{\sqrt{2}\Delta\omega} \right) u(\omega). \quad (42)$$

These modes $\{v_n(\omega)\}$ form an orthonormal basis of modes.

In order to describe the spectral phase up to the k^{th} order, one needs to use the basis $\{v_n(\omega)\}$ up to the mode k . In this paper, we develop the spectral phase to the second order; therefore, we use the following modes:

$$v_0(\omega) = i u(\omega) \quad (43)$$

$$v_1(\omega) = i \frac{\omega - \omega_0}{\Delta\omega} u(\omega) \quad (44)$$

$$v_2(\omega) = i \frac{1}{\sqrt{2}} \left(\frac{(\omega - \omega_0)^2}{\Delta\omega^2} - 1 \right) u(\omega). \quad (45)$$

The mode spectral profiles are plotted in Figure 5.

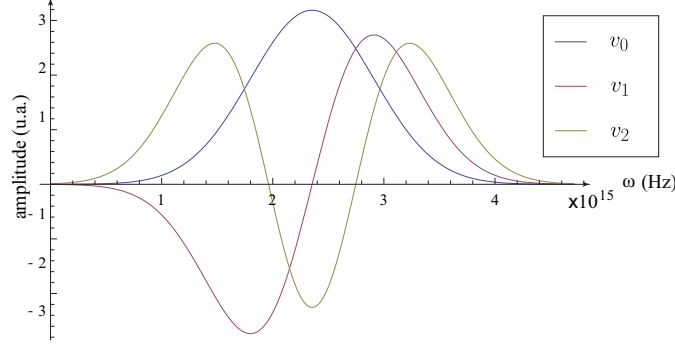


Fig. 5. Spectral profile of Hermite-Gaussian modes v_0 , v_1 and v_2 .

C. Detection modes of environmental parameters

Detection modes read :

$$\begin{aligned}
 w_L(\omega) &= \frac{1}{cK_L} (\omega_0 v_0(\omega) + \Delta\omega v_1(\omega)) \\
 w_X(\omega) &= \frac{LK(\omega_0)}{cK_X} \left[\left(\omega_0 + \frac{\Delta\omega^2}{\omega_0} (\delta_1 + \delta_2) \right) v_0(\omega) + \Delta\omega (1 + \delta_1) v_1(\omega) + \sqrt{2} \frac{\Delta\omega^2}{\omega_0} (\delta_1 + \delta_2) v_2(\omega) \right] \\
 w_{P_w}(\omega) &= \frac{-Lg(\omega_0)}{cK_{P_w}} \left[\left(\omega_0 + \frac{\Delta\omega^2}{\omega_0} (\eta_1 + \eta_2) \right) v_0(\omega) + \Delta\omega (1 + \eta_1) v_1(\omega) + \sqrt{2} \frac{\Delta\omega^2}{\omega_0} (\eta_1 + \eta_2) v_2(\omega) \right]
 \end{aligned} \tag{46}$$

where we have defined characteristic quantities that do not depend on the environmental parameters T , P , x and P_w :

$$\delta_1 = \omega_0 \frac{K'(\omega_0)}{K(\omega_0)}, \quad \delta_2 = \frac{\omega_0^2}{2} \frac{K''(\omega_0)}{K(\omega_0)}, \tag{47}$$

$$\eta_1 = \omega_0 \frac{g'(\omega_0)}{g(\omega_0)}, \quad \eta_2 = \frac{\omega_0^2}{2} \frac{g''(\omega_0)}{g(\omega_0)}. \tag{48}$$

Defining :

$$K_L = \frac{1}{c} \sqrt{\omega_0^2 + \Delta\omega^2} \tag{49}$$

$$K_X = \frac{K(\omega_0)L}{c} \sqrt{\left(\omega_0 + \frac{\Delta\omega^2}{\omega_0} (\delta_1 + \delta_2) \right)^2 + \Delta\omega^2 (1 + \delta_1)^2 + 2 \frac{\Delta\omega^4}{\omega_0^2} (\delta_1 + \delta_2)^2} \tag{50}$$

$$K_{P_w} = \frac{g(\omega_0)L}{c} \sqrt{\left(\omega_0 + \frac{\Delta\omega^2}{\omega_0} (\eta_1 + \eta_2) \right)^2 + \Delta\omega^2 (1 + \eta_1)^2 + 2 \frac{\Delta\omega^4}{\omega_0^2} (\eta_1 + \eta_2)^2} \tag{51}$$

Measurements with the detection modes give:

$$M[w_L] = p_L + \frac{K_X}{K_L} \langle w_L, w_X \rangle p_X + \frac{K_{P_w}}{K_L} \langle w_L, w_{P_w} \rangle p_{P_w} \tag{52}$$

$$M[w_X] = \frac{K_L}{K_X} \langle w_L, w_X \rangle p_L + p_X + \frac{K_{P_w}}{K_X} \langle w_L, w_{P_w} \rangle p_{P_w} \tag{53}$$

$$M[w_{P_w}] = \frac{K_L}{K_{P_w}} \langle w_L, w_{P_w} \rangle p_L + \frac{K_X}{K_{P_w}} \langle w_X, w_{P_w} \rangle p_X + p_{P_w} \tag{54}$$

Calculation of the purified mode w_L^p : we first calculate a orthonormal basis in the plane $\{w_X, w_{P_w}\}$, which leads for example to a basis $\{w_X, w_{P_w}^i\}$ where

$$w_{P_w}^i(\omega) = \frac{1}{\sqrt{1 - \langle w_X, w_{P_w} \rangle^2}} (w_{P_w}(\omega) - \langle w_X, w_{P_w} \rangle w_X) \quad (55)$$

Then we do a Gram-Schmidt orthonormalization of $\{w_X, w_{P_w}^i, w_L\}$ which gives:

$$w_L^p(\omega) \propto w_L(\omega) - \langle w_L, w_X \rangle w_X(\omega) - \langle w_L, w_{P_w}^i \rangle w_{P_w}^i \quad (56)$$

The normalization constant is:

$$\sqrt{1 - \frac{\langle w_L, w_{P_w} \rangle^2 + \langle w_L, w_X \rangle^2 - 2\langle w_L, w_{P_w} \rangle \langle w_L, w_X \rangle \langle w_X, w_{P_w} \rangle}{1 - \langle w_X, w_{P_w} \rangle^2}} \quad (57)$$

Acknowledgments

The research is supported by ANR project Qualitime, ERC starting grant Frecquam and by the Australian Research Council Centre of Excellence for Quantum Computation and Communication Technology, project number CE110001027 (OP).